Acta Montanistica Slovaca
ISSN 1335-1788
actamont.tuke.sk

Design of a real-time control algorithm for efficient small-diameter rock drilling

Edita LAZAROVÁ[1], Ví'azoslav KRÚPA[2], Mária BALI HUDÁKOVÁ[3], Alexander KIOVSKÝ[4], Pavol VAVREK[5] and Lucia IVANIČOVÁ[6]*

Authors' affiliations and addresses:
[1-6] Institute of Geotechnics, Slovak Academy of Sciences, Watsonova 45, 040 01 Košice, Slovakia
[1] e-mail: lazarova@saske.sk
[2] e-mail: krupa@saske.s
[3] e-mail: krulakova@saske.sk
[4] e-mail: kiovsky@saske.sk
[5] e-mail: vavrek@saske.sk
[6] e-mail: ivanic@saske.sk

***Correspondence:**
Edita Lazarová, Institute of Geotechnics, Slovak Academy of Sciences, Watsonova 45, 040 01 Košice, Slovakia
tel.:+421 55 792 2642
e-mail: lazarova@saske.sk

Funding information:
VEGA 2/0090/23
APVV 23-0364

Acknowledgement: This work was supported by the project VEGA 2/0090/23 and APVV-23-0364.

How to cite this article:
Lazarová, E., Krúpa, V., Bali Hudáková, M., Kiovský, A., Vavrek, P. and Ivaničová, L. (2026) Design of a real-time control algorithm for efficient small-diameter rock drilling. *Acta Montanistica Slovaca,* Volume 31 (1), 249-265

DOI:
https://doi.org/10.46544/AMS.v31i1.19

Abstract
The article presents a methodology for determining the relevant parameters defining the rock drilling process and their use in a real-time algorithm for efficient control of small-diameter rock drilling with diamond core bits. For this purpose, a series of experiments was performed on a horizontal laboratory drilling rig equipped with a complex measurement system. The results of experimental measurements, the identification of variables, and the expression of relationships between them form the basis for derived mathematical models that calculate the limit values of thrust force and penetration depth, delimiting the drilling zone with minimal energy consumption. Our research has shown the simplicity of drilling optimisation in terms of specific energy. The proposed optimisation is based on a controlled change of the thrust force. The control intervention – increasing the thrust force - is carried out if the measured penetration depth is outside the calculated interval defining the zone of efficient drilling. Comparison of the calculated specific energy values showed that drilling with forces outside the specified penetration-depth interval resulted in a significant increase in specific energy.
The proposed flexible and adaptive real-time optimisation algorithm, based on experimental findings, provides a theoretical framework for efficient small-diameter drilling into strong to very strong rocks, using a single controlled variable - penetration depth.

Keywords
rock drilling, measurement while drilling, online monitoring system, process efficiency, optimisation

Introduction

Rotary drilling is an energy-intensive operation widely used in mining and underground engineering, and as such, it is a complex technological process with complex relationships among its parameters. To accurately determine the factors that enter the drilling process and identify their impact on rock-breaking efficiency, the drilling process was subjected to experimental research. The studies on rock breaking by drilling, performed in laboratory conditions, improve our understanding of the interactions between the drilled rock and the drilling tools, and provide the information necessary for evaluation and optimal control of the drilling process in terms of the drilling performance and energy demands, which may significantly reduce the costs of drilling operations.

The rock drilling performance is affected by the constructional and performance parameters of the drilling equipment and the drill bit, the parameters related to the drilling process, including the weight on bit – thrust force, rotation speed, flushing fluid flow characteristics, and the parameters related to the properties of the drilled rock, such as rate of penetration, rotation torque, flushing fluid pressure, induced vibrations (Bhatnagar et al., 2011; Li et al., 2020; Yassien et al., 2020; Sakiz et al., 2022). For evaluation of the impact of changes in various combinations of the operational parameters on the potential operational and cost benefits of the drilling operations, multiple studies have been performed (Davarpanah et al., 2020; Hankins et al., 2015; Huang and Wang, 1997; Tang et al., 2017; Wang and Salehi, 2015). The tests were based on the mode that controls the drilling parameters – the drilling rate, the drill rotation speed, the torque, and the thrust force. These parameters are monitored during the drilling process.

Numerous on-site and laboratory drilling tests have shown that drilling parameters and rock mechanical parameters are closely related (He et al., 2020; Singh et al., 2012). Based on systematic studies, correlation models have been derived between rock compressive strength and drilling parameters (Feng et al., 2020; Kalantari et al., 2018). Authors of the paper (He et al., 2020; Kalantari et al., 2019) identified relationships between rock strength parameters and operational drilling parameters based on the geometry of the drilling tools. The impact of drill bit wear on drilling efficiency was examined, and methodologies for the indirect identification of wear degree were developed (Mostofi et al., 2018; Perez et al., 2017a). The correlation between the bit wear and the noise emission was identified (Eaton et al., 2023; Klaic et al., 2018; Wang et al., 2020). Based on changes in the curves of vibro-acoustic signals, it was possible to detect an imminent bit failure (Flegner et al., 2019; Karakus and Perez, 2014; Lazarová et al., 2020).

In the case that the thrust force, the flushing fluid flow, and the rotation speed are kept relatively constant during drilling, then the calculated values of the rate of penetration enable the detection of changes in lithology, changes in the rock strength parameters, or the presence of anomalies, such as micro-cavities and fractures. The rate of penetration is closely related to rock-breaking efficiency (Perez et al., 2017b). Multiple research studies have therefore been conducted to develop models for the effective prediction and optimisation of the rate of penetration (Hassan et al., 2020; Hegde et al., 2019; Shishavan et al., 2015). Over the last decade, the rate of penetration has been predicted primarily using machine learning technologies (Soares and Gray, 2019).

Oydere and Gray (2020) focused their research on optimising the drilling process based on the predictions of the torque, which is the key element in the calculations of the energy requirement for rock breaking. They modelled the torque as a function of the rotation speed, weight on bit, flow rate, pump pressure, and unconfined compressive strength. They used machine learning technologies to predict and optimise the torque. Authors of the papers Khosravanian et al. (2016) and Ma et al. (2023) investigated the use of the weight-on-bit parameter in designing a system for controlling the drilling process.

The quantification of drilling efficiency, conducted in research laboratories, in laboratories for testing drilling tools, and in situ, is based on specific energy. In rock cutting and drilling, specific energy is the energy required to break a unit volume of rock, and it is a crucial indicator for calculating rock-cutting/drilling efficiency and quantitatively assessing rock-breaking efficiency. Sensors on the drill rig systematically record the main drilling parameters – thrust, torque, rate of penetration, and rotation speed, from which the specific energy can be easily derived. Specific energy depends on drilling speed, thrust force, rotation speed, rock strength, and fluid flow during drilling operations (Al-Sudani, 2017; Babaei Khorzoughi and Hall, 2016; Chen et al., 2016; Pessier & Fear, 1992). In the paper by Al-Sudani (2017), a new, simple, and accurate method was presented for analysing drilling efficiency by calculating the transferred mechanical energy as a function of real-time bit wear, to achieve cost-effective drilling. Optimising specific energy can reduce time-consuming processes, lower costs, and improve drilling performance, thereby increasing the rate of penetration (Chen et al., 2014; Guo et al., 2021).

Apparently, the drilling performance is affected by many factors. However, including a large number of variables in a mathematical model is very difficult and inaccurate. The existing models often apply to a specific type of drilling system and to a specific control strategy for drilling variables. If any of those variables change during the drilling, the model's applicability is disputable.

The purpose of the presented research was to develop an innovative methodology for the complex monitoring, measurement, and acquisition of key drilling parameters; data analysis; and drilling process assessment. Subsequently, based on the designed methodology, a new approach for real-time drilling optimisation targeting

the minimum specific energy was verified in laboratory conditions. The designed algorithm enables reducing energy consumption in the drilling process by controlling a single variable - penetration depth.

Core drilling of rocks

Core drilling of rocks is fundamental to exploratory drilling. It is mainly used in mining geology, the geological survey of mineral deposits, the exploration of oil and natural gas deposits, and engineering geological prospecting during the foundation of structures and injection wells. A characteristic of core drilling is that the destruction of the rock is not carried out along the entire borehole cross-section, but only along the circumference of the annular contour, while the rock remains in its original state in the centre of the borehole. The undamaged part of the borehole – the core - enables continuous, direct visual geological documentation of the entire borehole and provides the basis for determining the rock's physical, mechanical, and technological properties and for petrographic analysis of the rock environment. Diamond or carbide core drill bits are used for core drilling.

In the presented experimental research, surface-set diamond core drill bits of the outer diameter of 46 mm (usually used in mining, engineering-geological prospecting, and construction engineering for small-diameter exploratory drilling operations) were tested and analysed. In surface-set diamond bits, a layer of diamond grains embedded in the bit matrix is primarily responsible for rock failure during drilling. The diamonds are in contact with the rock surface during drilling and are subjected to high pressures induced by the thrust force acting on them. Two forces act on each diamond that is set in the matrix of the bit's cutting segment: a normal force that causes crushing of the rock under the diamond, and a rotational force, which causes splitting of rock chips. The overall breaking mechanism under the drill bit is the sum of the individual effects of all the active diamond grains of the bit that are in actual contact with the rock surface. The concentration of diamonds on the bit surface affects the wear of the whole bit matrix. A higher concentration of diamonds protects the bit matrix better and thus increases the drill bit's lifetime.

The core drilling systems are characterised by a compact structure, small dimensions, and a low weight. They facilitate highly accurate, relatively short-lasting drilling of thin boreholes to great depth. Core drilling is characterised by high work intensity, low profits, and a low degree of automation (Lin et al., 2012). Drilling efficiency is primarily determined by the expertise, experience, and intuition of the operators who control the drilling system's operational parameters and intervene in the control system to optimise drilling conditions.

At present, investments are made into the research and development of autonomous and smart drilling systems. The systems for the automation of drilling must be highly accurate and reliable, able to promptly choose the best procedure in case of an unpredictable situation during the drilling, which might escalate hazards for operators, the surrounding environment, and the expensive equipment (Downton, 2012; Godhavn et al., 2011; Khadisov et al., 2020; Meng et al., 2012).

Research procedure and data collection

The data monitored during the in situ drilling are affected by a number of external and internal factors and conditions. To investigate diamond core drilling, a series of experiments was performed on a horizontal laboratory drill rig, using equipment to simulate a real-life drilling process without the impact of the drill string.

Experimental equipment and measuring system

The experimental drill rig was designed and constructed at the Institute of Geotechnics of the Slovak Academy of Sciences, Kosice, Slovakia, and it serves for the following purposes:

- Examination of the effect of a drilling mode on the course of the rock breaking process;
- Research on the rock drillability;
- Study of the energy consumption for the drilling process.
- Investigation of vibration signal generated during rock drilling.

The equipment is equipped with a dedicated online measurement system, which:

- Controls and monitors the experiment;
- Provides the measured values of the process parameters in the form of changes over time;
- Enables the online visualisation of the torque and three orthogonal components of cutting forces;
- Provides the values and visualisation of the vibration acceleration in three orthogonal directions;
- Provides the online parameter values calculated from the monitored data using the pre-defined equations.

The experimental drill rig with its main parts is shown in Figure 1. The thrust force acting on the rock was continuously controlled and measured by a pressure cell at the hydraulic cylinder (5). The rotation speed of the drill bit (6) was controlled by regulating the electromotor (3). The torque and three orthogonal components of the cutting force were measured by a 4-component dynamometer (10). The drilled length was measured by a

magnetostrictive linear position sensor installed at the hydraulic cylinder, with an accuracy of 10 μm (4). The terminal switch of the position measurement enabled drilling to a maximum depth of 260 mm into a rock specimen. The thrust force, drilled length, rotation speed, and torque were measured at a sampling frequency of 100 Hz. The fixing frame (8) of the test rock specimen (7) was used to firmly attach the piezoelectric accelerometers (9) in 3 orthogonal directions, with online vibration monitoring via the system at a sampling frequency of 18 kHz. The hose (1) attached to the water pump was used to supply the drilling fluid to the drill bit at a constant flow rate of 10^{-3} $m^3.s^{-1}$.

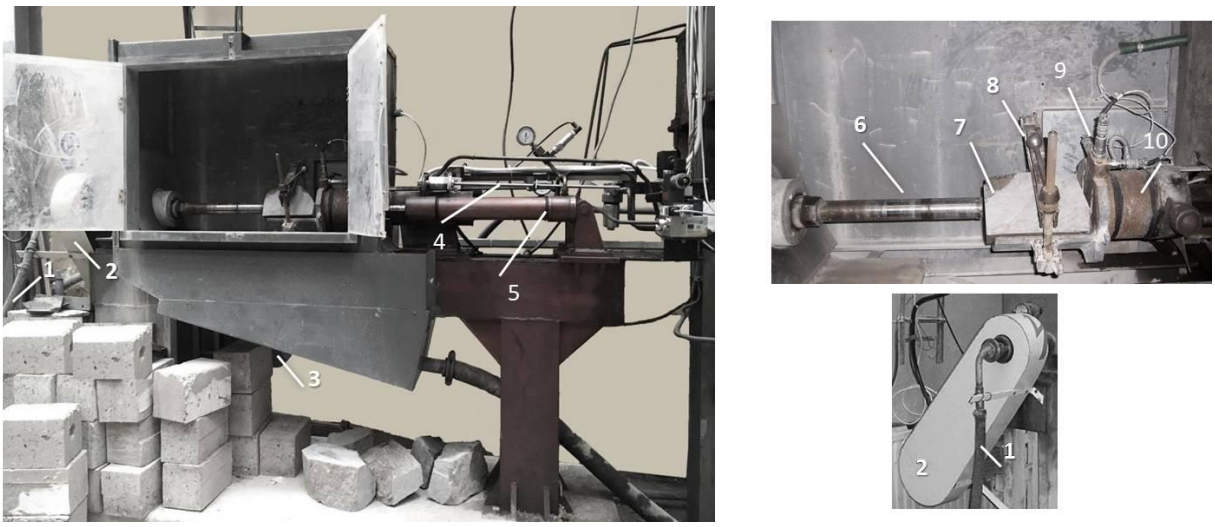

Fig. 1. Experimental drill rig and its main parts: 1 – drilling fluid supply hose; 2 – belt drive; 3 – electromotor; 4 – magnetostrictive linear position sensor; 5 – double-acting hydraulic cylinders; 6 – core barrel with the drill bit; 7 – rock specimen; 8 – rock specimen fixing frame; 9 – accelerometers; 10 – 4-component dynamometer

The drill rig was controlled by the computer in automatic mode. The measured data were sent to and stored on the archive server. The operational ranges of the laboratory drill rig are listed in Table 1.

Table 1 Applicable ranges of the laboratory drilling rig mode parameters

Rotation speed n (rpm)	Thrust force F (kN)	Drilled length L (m)	Flushing fluid flow rate ($m^3.s^{-1}$)
≤ 2,220	≤ 20	≤ 0.26	10^{-3}

The scheme in Figure 2 shows the information flow for the acquisition and transmission of data to the required place within the required time, as well as the connections between the individual units of the technical equipment. The essential core of the entire measuring and control system is the control computer PC1, which allows to plan, start, or stop the drilling process; sets the values of the input variables – thrust force, drill bit revolutions, drilled depth; continuously monitors the technical condition of the drill rig; ensures the measurement and recording of the electric motor revolutions, hydraulic pressure of the rig, torque, and drilled depth; provides the acquisition of vibration acceleration values measured in three orthogonal directions from the Adash vibration monitoring system; and provides the acquisition of torque values and three orthogonal components of the cutting force from the Kistler system. The drill rig's actual operation is ensured by an industrial PLC that also includes an OPC server. The application program in the PLC allows control of the drill rig online, automatically from the control PC1 via Ethernet OPC communication, or manually via mechanical switches and a touchscreen. The communication between the PC1 and the industrial PLC computer uses Ethernet OPC. The PC1 generates a trigger pulse via the PCA-7428AL converter to initiate synchronous measurement of force components via the Kistler system on the PC2. The PC1 also ensures that measured data are written to the data server.

The drill rig is equipped with a 23 kW electric motor that drives the drill bit rotation. The electric motor is controlled by an inverter drive connected to the PLC via a Profinet network. At the same time, the inverter sends the sensed speed and torque values at 100 Hz to the PLC. The drilled depth is measured using the magnetostrictive linear position sensor Baluff BTL7 Micropulse Transducer, with an accuracy of 10 μm and a scanning frequency of 100 Hz. Its signal is transmitted to the PLC via the I/O module. The thrust force acting on the rock is generated by a hydraulic unit controlled by a proportional control valve system. The hydrogenerator is controlled from the PLC via the I/O module. The applied pressure value is transmitted via the I/O module to the PLC. Piezoelectric vibration sensors Wilcoxon 784A-3 and CTC AC102-1A, with different sensitivities and resonance frequencies of 18 kHz, are used for vibration measurement, along with the online vibration monitoring system Adash 3900-II.

The processed signals are transmitted by the transceiver through the AD converter PCA-7428AL and written to the control computer PC1. The PLC also controls the flushing fluid pump.

The PC2 computer serves as a dedicated setting, starting and controlling the measurement of force components and torque using Kistler DynoWare software, with the option to graphically display the time course of the measured values. A 4-component dynamometer, Kistler 9272, along with a multichannel charge amplifier for multicomponent force measurement, Kistler 5070 (100 Hz sampling frequency), is used for the precise force measurement. The processed signals are transferred from the amplifier via the PCMCIA AD converter to the PC2.

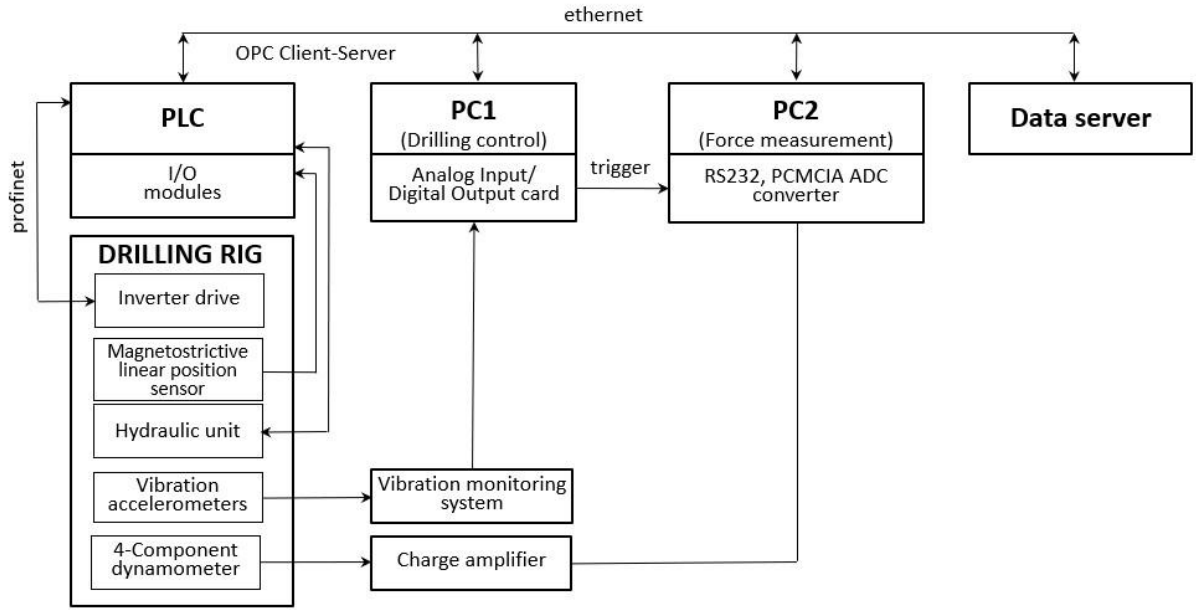

Fig. 2. Detailed diagram of the data information flow

Tested rock characteristics

It is necessary to consider that the rock, no matter how homogeneous appearing, is an anisotropic material with locally changing properties, which is manifested during its drilling. To account for the size effect of the diamond grains in the drill bit, it was necessary to choose a quasi-homogeneous rock suitable for drilling with surface-set diamond bits, which in this case was a solid andesite. The test specimens were purchased from a local andesite quarry and cut into blocks approximately 150x150x300 mm using a circular saw.

Fig. 3. Specimens of the drilled andesite (left – rock specimen, middle – drilled core, right – microscopic image of andesite surface at 80x magnification)

The tested rock was andesite from a quarry in Ruskov, Slovakia. The quarry bed consists of massive, intensively cracked, small- to medium-grained pyroxene andesite of grey to dark-grey colour, which naturally breaks into irregular or large blocks and shows only scant parting into thick slices. Macroscopically, andesite is of a porphyritic structure with plagioclase outgrowths. Cracks are mostly filled with secondary iron minerals. In exceptional cases, the rock in the deposit is porous or even cavernous. The specimen of the drilled andesite, the drilled core, and a detailed image of the specimen at an 80-fold magnification are shown in Figure 3. The tested andesite was a moderately abrasive rock with a Cerchar abrasivity index of 3.05 and a strong rock with an uniaxial compressive strength of 293.8 MPa. These properties were identified in accordance with the applicable standards CEN ISO/TS 17892, EN 1997–2:2007(E), and ON 441121.

Tested drill bit characteristics

The surface-set core drill bits are primarily intended for the water-flushed exploratory drilling into soft, medium-soft, hard, or very hard rocks, and for the collection of specimens from a drilled core for the constructional, geophysical, and geological purposes. They are characterised by a high hardness, good wear resistance, a simple structure, and a flexible design. When used, they exhibit good performance, a long service life, high penetration rates, and good stability.

To assess and analyse the effect of different diamond grain sizes on drilling efficiency, three small-diameter surface-set diamond drill bits with a simple core and varying diamond grain sizes were selected for the experimental research presented. All three bits had the same geometry, diameter, number of cutting segments, and matrix quality. The only difference was the size of the individual diamond grains set in the bit matrix (specified in the manufacturer's technical documentation as the number of diamond grains per carat, or gram). The parameters of the tested drill bits manufactured by Urdiamant, s.r.o., Czech Republic, are shown in Table 2.

Table 2 Parameters of the surface-set diamond drill bits used in the experiments

Drill bit		Type 12/18	Type 16/25	Type 25/35
Size of diamond grains defined as:	stones per carat	12-18	16-25	25-35
	stones per gram	60-90	80-125	125-175
	calculated diamond size (mm)	2.08-1.82	1.89-1.63	1.63-1.46
Number of cutting segments		4		
Outer diameter		46 mm		
Core diameter		32 mm		
Matrix hardness		400 HV		

Research methodology

For research purposes, the experimental drilling setup was designed for the acquisition and recording of the input control parameters of the experimental series: thrust force F (kN) and rotation speed n (rpm); and the output process parameters: penetration depth p (mm) and torque T (Nm). The recorded data were processed and analysed offline using the software for numerical calculations, modelling, design of algorithms, data analysis, and visual presentation (Matlab) and Microsoft Excel. The next step was to design and develop mathematical models to calculate the limit values defining the zone of efficient drilling. The solution yields a flexible, adaptive optimisation algorithm for controlling core drilling with surface-set diamond drill bits. The applied research methodology setup is presented in Figure 4.

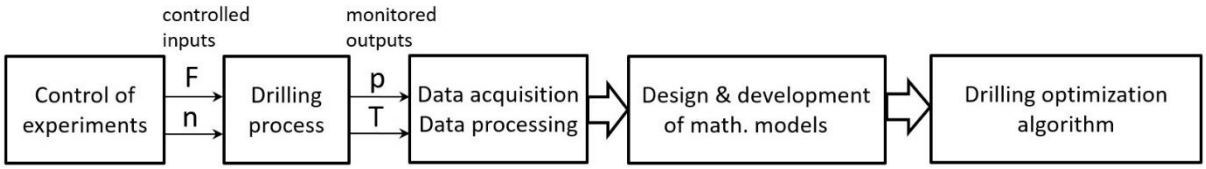

Fig. 4. Concept of the research methodology; F (N) - thrust force, n (rpm) - rotation speed, T (Nm) - torque, p (mm) - penetration depth

Ten series of four drilling experiments were performed for each of three tested drill bit types (12/18, 16/25, 25/35). All four series were drilled at gradually increasing thrust force from 0 to 20 kN at four preset levels of drill bit rotation speed (800, 1,000, 1,200, and 1,400 rpm). The rotation speed levels were selected based on the manufacturer's recommendations for the tested drill bits (Urdiamant, s.r.o., Czech Republic). Drilling experiments were carried out at a quasi-constant flushing fluid (water) flow rate sufficient to clean the borehole face. During each experiment, approximately 0.26 m of andesite specimen was drilled. The input parameters for the experiments are shown in Figure 5, along with detailed photos of the cutting segments of the tested drill bits, showing the different diamond grain sizes.

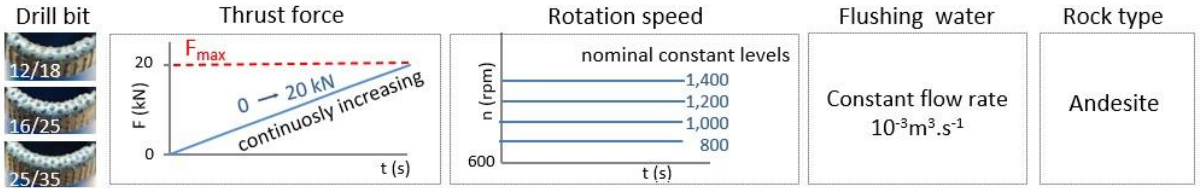

Fig. 5. Setup of experiments

Calculations of the efficient drilling zone

An alternative, generally accepted approach to characterising the drilling process from an energy perspective is the concept of specific energy (SE), introduced by Teale (1965). In rock cutting, specific energy is the energy consumed to break a unit volume of rock, serving as a crucial indicator for calculating rock cutting efficiency and as a quantitative measure of it. The basic equation used for the calculation of specific energy follows:

$$SE = \frac{W}{V} = \frac{2\pi.T}{A.p} \qquad (MJ.m^{-3}) \tag{1}$$

where W (J) is the energy consumed in rock breaking, and V (m^3) is the volume of the broken rock; T (Nm) is the torque; A (m^2) is the surface area of the contact between the bit and the rock; p (m) is the penetration depth.

Continuous theoretical and experimental research into mechanical rock breaking provided additional knowledge that facilitated more accurate identification of equations for calculating specific energy by applying physical laws and making mathematical adjustments (Deng et al., 2022; Hassan et al., 2020; Zhou et al., 2017). In this study, the following equation was used:

$$SE = \frac{F}{A} + \frac{2\pi}{A}.\frac{T}{p} \qquad (MJ.m^{-3}) \tag{2}$$

where F (N) is the thrust force; p (m) is the penetration depth; T (Nm) is the torque; A (m^2) is the surface area of the contact between the tool and the rock.

The first member of the equation $\frac{F}{A}$ represents the contribution of the thrust force component, equivalent to the pressure acting over the borehole's cross-sectional area, and accounts for approximately 1.5% of the total specific energy. From the physical point of view, it defines the magnitude of the energy required for the rock deformation and for the rock breaking processes related to the formation of starter cracks, the crack propagation, and the subsequent macroscopic violation of the rock's structural integrity. It also creates the required pre-breaking stress in the zone where the diamonds contact the rock, as well as the conditions for initiating rock-breaking. However, it has no significant effect on the total value of specific energy.

The second member $\frac{2\pi}{A}.\frac{T}{p}$ is the rotary component of energy (torque). Energy resulting from torque constitutes the major part of the drilling-specific energy. The fraction $\frac{2\pi}{A}$ in the equation is constant for the given drill bit and depends on the contact area between the bit and the rock. The applied drilling mode only affects the $\frac{T}{p}$ fraction.

The goal of the following mathematical modelling was to develop an innovative analytical solution for torque and penetration depth that can determine the zone of efficient drilling.

Torque T (Nm) is almost linearly dependent on the thrust force F (N), Figure 6.

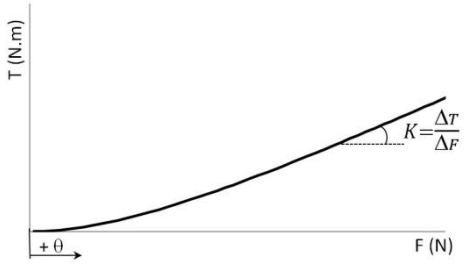

Fig. 6. Graphical representation of the T(F) dependence; as defined by Eq.(3)

An innovative mathematical model of the torque as a function of the thrust force was derived:

$$T = \kappa\left[F + \theta\left(e^{-\frac{F}{\theta}} - 1\right)\right] = \kappa.F + \kappa.\theta.e^{-\frac{F}{\theta}} - \kappa.\theta \quad (N.m) \tag{3}$$

wherein F (N) is the applied thrust force. Substitution coefficient κ (mm) expresses a linear response of the torque to the growing thrust force; θ (N) represents a delay in the response of the drilling set at low thrust force values.

For the linear section of the torque curve, where F>4.θ, the torque T (N.m) is calculated using the following equation:

$$T = \kappa(F - \theta) \quad (N.m) \tag{4}$$

The mathematical expression of the curve p as a function of the thrust force *F* was then described by the following derived formula (Blišťan, 1999; Krupa et al., 2018):

$$p = p_{max}[1 - e^{-\omega.F}(1 + \omega.F)] = p_{max}(1 - e^{-\omega.F}) - p_{max}.\omega.F.e^{-\omega.F} \quad (mm) \tag{5}$$

where p_{max} (mm) is the maximum penetration depth to which the equation's solution converges, and ω (N^{-1}) is the substitution coefficient. Through gradual derivations of Eq.(5) based on the thrust force, the following equations were derived:

$$\frac{d^2p}{dF^2} = p_{max}.\omega^2.e^{-\omega.F}(1 - \omega.F) \tag{6}$$

$$\frac{d^3p}{dF^3} = p_{max}.\omega^3.e^{-\omega F}(\omega.F - 2). \tag{7}$$

Through further mathematical adjustments, it was observed that:

- The value of the thrust force in the inflexion point F_{inf} of the p(F) curve was inverse to the value of the substitution coefficient ω:

$$\frac{d^2p}{dF^2} = 0 \rightarrow F_{inf} = \frac{1}{\omega} \quad (N). \tag{8}$$

  The highest probability of efficient drilling occurs near the inflexion point F_{inf} of the penetration-thrust curve (Krupa et al., 2018). Energy theories of rock breaking assume that in this zone of F_{inf}, the energy necessary to break the unit volume of rock (i.e., specific energy) reaches its minimum. The thrust force F_{inf} delimited the lower boundary of that zone of efficient drilling.
- The most pronounced deceleration in the increase in penetration depth was observed at the F_{up} thrust force, which was twice the F_{inf} value. The thrust force F_{up} delimited the upper boundary of the zone of efficient drilling:

$$\frac{d^3p}{dF^3} = 0 \rightarrow F_{up} = \frac{2}{\omega} = 2F_{inf} \quad (N). \tag{9}$$

Figure 7 shows a curve of the dependence of the penetration depth on thrust force, with boundary thrust force values F_{inf} and F_{up} delimiting the zone of efficient drilling.

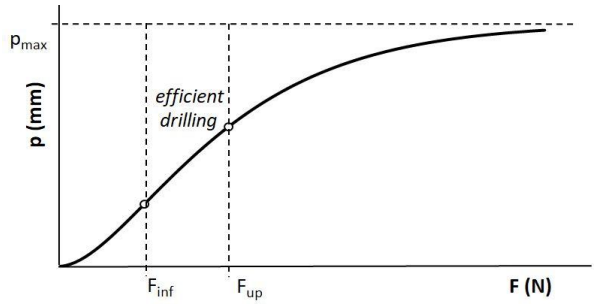

Fig. 7. Curve p(F) with boundary values F_{inf}, F_{up} delimiting the zone of efficient drilling

By substituting Eq.(3) and Eq.(5) in the above-discussed $\frac{T}{p}$ fraction, the resulting equation follows:

$$\frac{T}{p} = \frac{\kappa\left[F + \theta\left(e^{-\frac{F}{\theta}} - 1\right)\right]}{p_{max}\left[1 - e^{-\omega.F}(1 + \omega.F)\right]} \quad (N). \tag{10}$$

The first derivation of the function that equals zero was used to calculate the thrust force F_{opt} (N), as follows:

$$\frac{d\frac{T}{p}}{dF} = \frac{p\frac{dT}{dF} - T\frac{dp}{dF}}{p^2} = 0. \tag{11}$$

The function of specific energy reaches its minimum at the thrust force value F_{opt} (N). The resulting equation is as follows:

$$[1 - e^{-\omega.F}(1 + \omega.F)].\left(1 - e^{-\frac{F}{\Theta}}\right) - \left[F + \Theta\left(e^{-\frac{F}{\Theta}} - 1\right)\right]\omega^2.F.e^{-\omega.F} = 0. \quad (12)$$

For the linear part of the torque (F>4.Θ) in Figure 6, after the adjustments for the argument of the platform of specific energy $\frac{T}{p}$, the following simplified equation was derived:

$$e^{-\omega.F}(\Theta.\omega^2.F - \omega^2.F^2 - \omega.F - 1) + 1 = 0. \quad (13)$$

Figure 8 shows the correlation between the platform-specific energy $\frac{T}{p}$ and the thrust force.

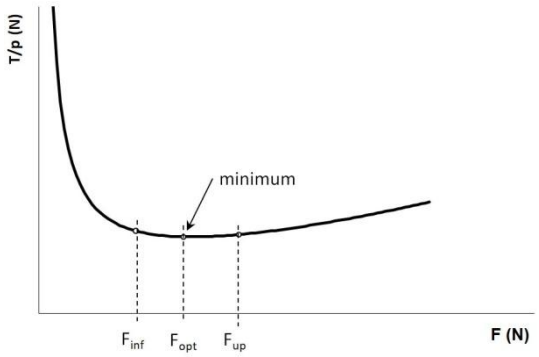

Fig. 8. Graph of the correlation between the platform of specific energy T/p and the thrust force F; lower boundary F_{inf} and upper boundary F_{up} of the efficient drilling zone, optimal thrust force F_{opt}

The argument of the minimum of the platform of specific energy $\frac{T}{p}$, identified by Eq.(10), is identical to the argument of the minimum of specific energy calculated by Eq.(2).

The derived mathematical models described in the results served their intended purpose. They allowed determining the optimal thrust force zone where efficient drilling occurs at minimum specific energy.

Results analysis

In total, 116 individual drilling experiments, making 30 m of drilled andesite samples, were performed by three tested drill bits. Experiments with different drilling modes, gradually increasing thrust force, and constant rotation speed were evaluated. The purpose of applying such non-conventional drilling conditions was to monitor, at a relatively short drilled length, changes in the interaction between the worn bit and the rock.

Mathematical models of T(F) in Eq. (3) and p(F) in Eq. (5) showed very high correlation between the experimental and theoretical values across all experiments, with correlation coefficients exceeding 0.97. As an example, the results from an experiment using a type 25/35 bit at 1,200 rpm with increasing thrust force are presented in Figure 9.

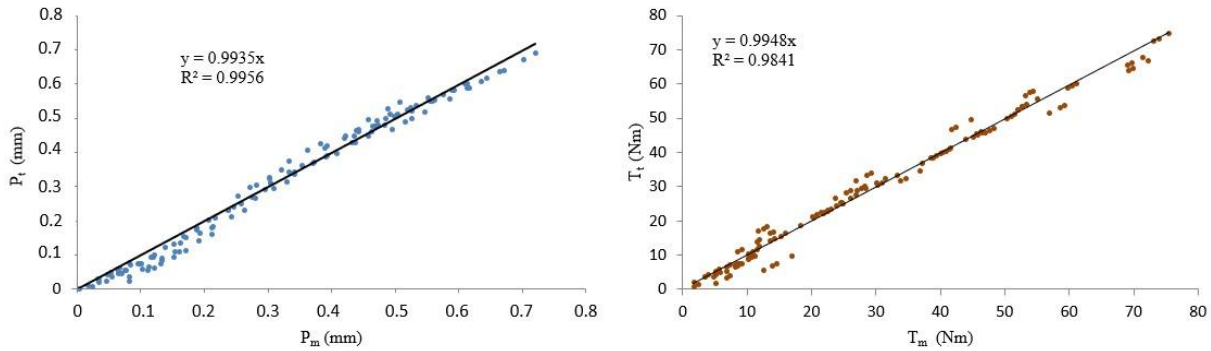

Fig. 9. Correlation between the experimental - p_m (mm), T_m (Nm), and theoretical - p_t (mm), T_t (Nm) values of penetration depth p (mm) and torque T (Nm); tested drill bit type 25/35, n=2000 rpm, increasing thrust force

The substitution coefficients of the derived mathematical models $T(F)$ and $p(F)$ were calculated in the Matlab environment by an algorithm based on the method of least squares, where the experimentally measured values were compared with the theoretical values of the derived models.

The mathematical models in Eq.(3), Eq.(5), and Eq.(10) were used to calculate the thrust force values that delimit the lower boundary F_{inf} and the upper boundary F_{up} of the zone of efficient drilling, as well as the thrust force F_{opt} at which the specific energy reaches the minimum value. The values F_{inf}, F_{up}, and F_{opt} were calculated for each experiment. Analysis showed that thrust forces increased with drilled length, following an exponential curve with $R2 \geq 0.7$ (Figure 10). From the plotted dependencies, it was clear that, in terms of the thrust force required for efficient drilling, there were significant differences among the drill bits used. The slowest increase of force values F_{inf}, F_{opt}, F_{up}, with drilled length exhibited at drilling with the drill bit type 12/18.

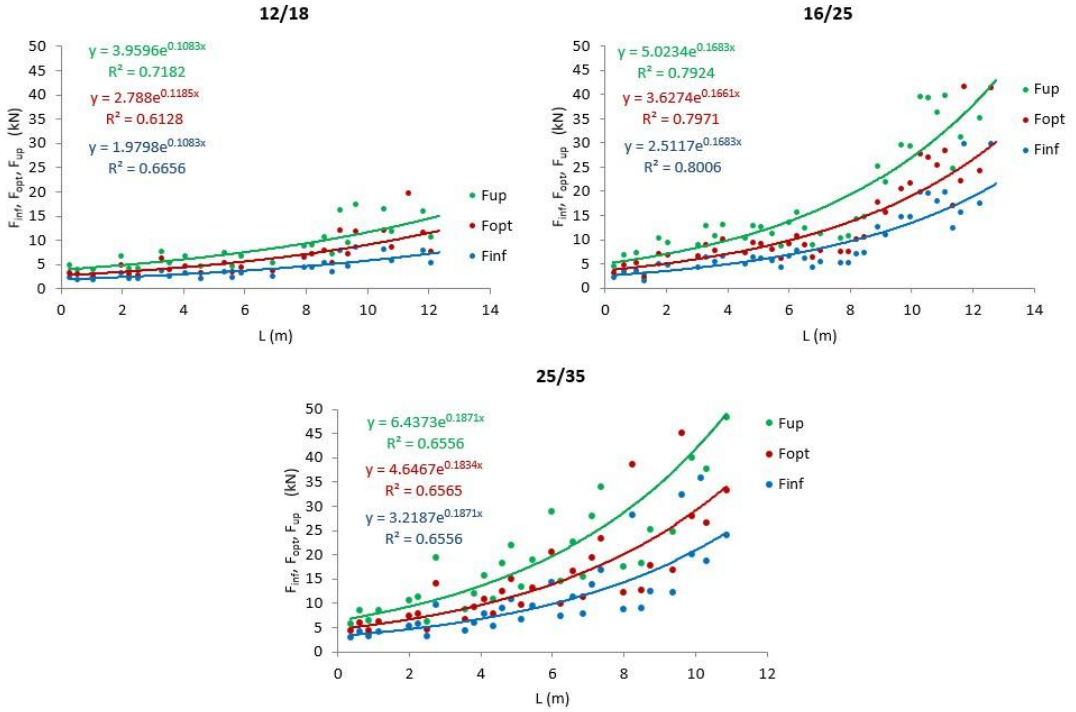

Fig. 10. Theoretical curves of the thrust force values in the zone of efficient rock drilling – F_{inf}, F_{opt}, F_{up}, depending on the drilled length for the tested drill bits.

Specific energy was calculated from the values measured during the experimental drilling. Figure 11 shows the experimentally measured specific energy values only in the efficient drilling zone, as a function of drilled length and applied thrust force. The specific energy outside that zone was much higher. The drawn curves clearly indicate a gradual increase in specific energy with increasing drilled length. A graphical representation in the plane defined by the F (kN) and L (m) axes corresponds to the curves shown in Figure 10; the drawn curves show a shift of the zone of efficient drilling toward higher thrust force values with increasing drilled length.

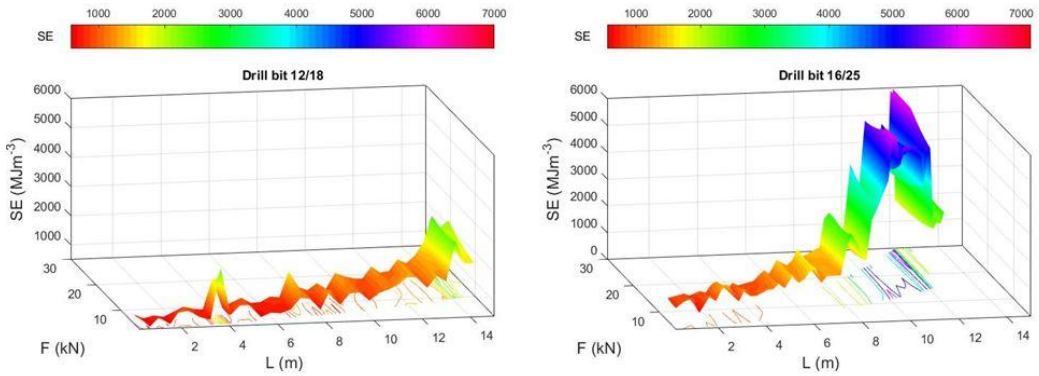

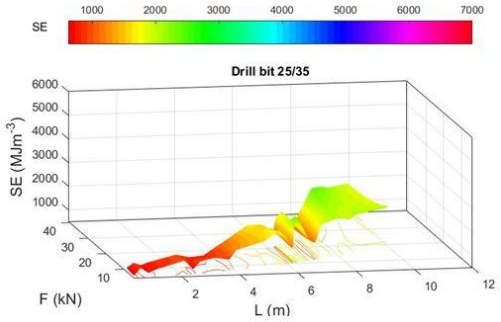

Fig. 11. Values of specific energy in the zone of efficient drilling calculated from experimental data

The specific energy values in Table 3 were calculated for the constant thrust forces F = 2.5, 5, 10, 15, and 20 kN, as well as for the optimal thrust force F_{opt}. Subsequently, the specific energy values were averaged over approximately 2 m of drilled andesite.

F_{opt} represents the thrust force where specific energy reaches its minimum and corresponds to the values calculated from Eq.(12). The parameter values ω and Θ were calculated for each individual experiment, i.e., drilled borehole. The values of these parameters reflect the progressive wear of the drill bit, resulting in a decline in its cutting ability as the total length drilled by a single drill bit increases, as reflected in the gradually increasing specific energy.

Table 3 Changes in the mean values of specific energy with an increasing drilled length for three tested surface-set diamond drill bits

		Average values of $\overline{SE}$ (MJ.m^{-3}) at relevant thrust force level F (kN)					
Drill bit	L (m)	2.5	5	10	15	20	F_{opt}
type 12/18	0-2	884	**750**	924	1,245	1,616	**737**
	2-4	1,358	**1,008**	1,085	1,378	1,738	**957**
	4-6	913	**767**	906	1,196	1,543	**763**
	6-8	1,230	**1,071**	1,137	1,367	1,658	**948**
	8-10	1,869	1,300	**1,102**	1,167	1,324	**1,018**
	10-12	2,407	1,759	**1,492**	1,549	1,724	**1,452**
type 16/25	0-2	1,094	**871**	982	1,259	1,594	**829**
	2-4	1,463	1,113	**975**	1,033	1,165	**969**
	4-6	1,874	1,348	**1,165**	1,242	1,411	**1,170**
	6-8	2,576	1,751	**1,485**	1,585	1,808	**1,492**
	8-10	8,614	4,832	3,167	**2,817**	**2,806**	**2,705**
	10-12	16,562	9,469	5,956	4,948	**4,603**	**4,298**
type 25/35	0-2	1,035	**793**	813	990	1,227	**761**
	2-4	1,450	1,052	**902**	958	1,086	**836**
	4-6	3,398	2,189	1,609	**1,496**	1,524	**1,462**
	6-8	3,996	2,636	1,840	1,619	**1,573**	**1,496**
	8-10	7,951	4,404	2,676	2,162	**1,960**	**1,775**
	10-12	10,841	5,732	3,327	2,614	**2,324**	**2,022**

Note: The highlighted data in the table represent the specific energy values calculated for the relevant thrust force level, with the lowest difference from the minimum specific energy at the thrust force F_{opt}.

By comparing the specific energy values calculated for the optimal thrust force F_{opt} and the actually applied thrust force F, the SE values with the smallest difference were identified. These values are marked in grey in Table 3. From the highlighted values in the table, it shows that after drilling the boreholes to a total length of approximately 8 m, drill bit type 12/18 prefers a thrust force of approximately 5 kN for efficient drilling and approximately 10 kN in other sections. The drill bit type 16/25 prefers a thrust force of approximately 10 kN up to the drilled length of ca. 8 m. With increasing drilled length, the zone of efficient drilling shifted to a thrust force of 15 to 20 kN, accompanied by a substantial increase in specific energy due to sudden physical damage to the drill bit body. Initial drilling with a 25/35 bit at thrust forces of 5 kN and 10 kN becomes inefficient in terms of specific energy after 4 m of drilled length, and the drill bit requires a gradual increase in thrust force up to 20 kN. An increase in the applied thrust force is associated with a downgrade in the drilling capabilities of the drill bit due to its progressive wear.

Table 4 Average values of penetration depth $\overline{p_{opt}}$ in drilling with an optimal thrust force F_{opt} and average values of specific energy $\overline{SE}$ (MJ.m-3) for the specified drilled length intervals

drill bit		L (m)	
		0-8m	> 8m
type 12/18	$\overline{p_{opt}}$ (mm)	0.2816	0.3122
	F_{opt} (kN)	5	10
	$\overline{SE}$ (MJ.m^{-3})	851	1,235
type 16/25	$\overline{p_{opt}}$ (mm)	0.2243	0.1418
	F_{opt} (kN)	10	20
	$\overline{SE}$ (MJ.m^{-3})	1,115	3,502
type 25/35	$\overline{p_{opt}}$ (mm)	0.3427	0.348
	F_{opt} (kN)	15	20
	$\overline{SE}$ (MJ.m^{-3})	1,139	1,899

Table 4 shows the average values of penetration depth $\overline{p_{opt}}$ in drilling with an optimal thrust force F_{opt} and a value of minimum specific energy for the given drilled length intervals. Comparison of the three tested drill bits showed that, for drill bit type 16/25, while maintaining optimal conditions, a stepwise increase in thrust and specific energy, accompanied by a significant reduction in penetration depth, occurred due to sudden physical damage to the bit body. The increase in thrust force required to ensure efficient drilling was related to progressive wear in the case of both bit types 12/18 and 25/35, whereas in the case of bit type 16/25, it was related to its sudden damage.

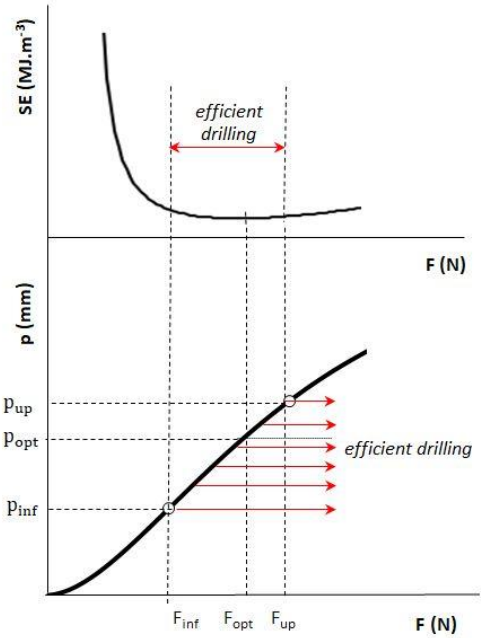

Fig.12. Boundary values thrust force and penetration depth delimiting the zone of efficient drilling with regard to the minimum values of specific energy.

The values of penetration depth p_{inf} at thrust force F_{inf} are calculated by entering Eq.(8) to Eq.(5):

$$p_{inf} = 0.264\, p_{max} \qquad (mm), \tag{14}$$

and at thrust force F_{up} by entering the Eq.(9) to Eq.(5):

$$p_{up} = 0.594\, p_{max} \qquad (mm). \tag{15}$$

The penetration depth at F_{opt} is defined by the following equation that was identified experimentally:

$$p_{opt} = 0.506\, p_{max} \qquad (mm). \tag{16}$$

The penetration depth ranges from ca 26% to 60% of the maximum penetration depth.

Based on a combination of theoretical knowledge, experimental results, and mathematical modelling, we have designed an algorithm for drilling with minimal energy consumption to control drilling with surface-set core diamond drill bits in real conditions. The designed algorithm, shown in Figure 13, assumes a gradual increase in thrust force at the start of drilling, which is automatically adjusted in the next step to achieve the first optimal thrust force, F_{up}. Drilling with the F_{up} will ensure the entire penetration depth is used within the efficient drilling zone. The penetration depth serves as the identification optimisation criterion. The algorithm checks online whether the measured penetration depth, p_m, lies within the efficient drilling zone. In case the identifying optimisation criterion ($p_m \in < p_{inf}; p_{up} >$) is not met, a new calculation is performed for the substitution coefficients from the p(F) curve, and of parameters p_{inf} and p_{up}. As soon as the thrust force F_{up} reaches the limit F_{max}, as determined by the equipment's technical conditions, the drilling process is completed.

The designed algorithm controls drilling efficiency by using penetration depth as a function of thrust force. Drilling with thrust force outside the calculated recommended penetration depth interval will cause a surge of specific energy.

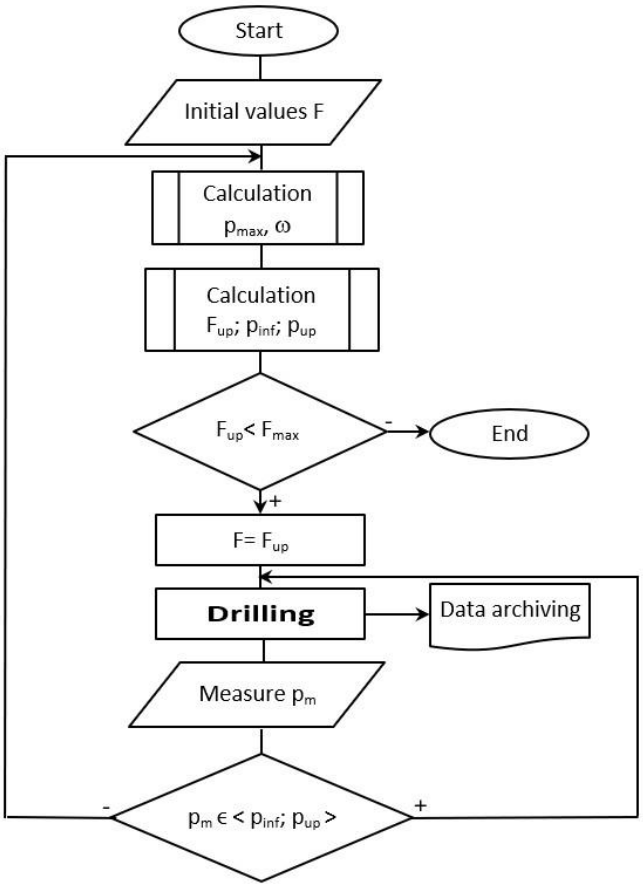

Fig. 13. Proposed algorithm designed for the optimisation of the drilling process

Table 5 shows the percentage deviation in specific energy when the recommended optimal thrust force is not maintained. The values were calculated by the formula:

$$\left(\frac{SE_F}{SE_{F_{opt}}} - 1\right).100 \qquad \% \tag{17}$$

from the experimental data presented in Table 3. The parameter SE_F (MJ.m^{-3}) represents the specific energy at the applied thrust force; SE_{Fopt} (MJ.m^{-3}) represents the specific energy at the optimal thrust force.

Table 5 Percentage deviation between specific energy SE_F and SE_{Fopt} in the case of not keeping the recommended optimal thrust force F_{opt}

		Percentage deviation of specific energy SE_F from SE_{Fopt} at actual applied thrust force F (kN)				
Drill bit	L (m)	2.5	5	10	15	20
type 12/18	0-2	19.9	**1.7**	25.4	68.9	119.3
	2-4	41.9	**5.3**	13.4	44.0	81.6
	4-6	19.7	**0.5**	18.7	56.7	102.2
	6-8	29.7	**13**	19.9	44.2	74.9
	8-10	83.6	27.7	**8.3**	14.6	30.1
	10-12	65.8	21.1	**2.8**	6.7	18.7
type 16/25	0-2	32.0	**5.1**	12.7	51.9	92.3
	2-4	51.0	14.9	**0.6**	6.6	20.2
	4-6	60.2	15.2	**0**	6.2	20.6
	6-8	72.7	17.4	**0**	6.2	21.2
	8-10	218.4	78.6	17.1	4.1	**3.7**
	10-12	285.3	120.3	38.6	15.1	**7.1**
type 25/35	0-2	36.0	**4.2**	6.8	30.1	61.2
	2-4	73.4	25.8	**7.9**	14.6	29.9
	4-6	132.4	49.7	14.6	**2.3**	4.2
	6-8	167.1	76.2	23.0	8.2	**5.1**
	8-10	347.9	148.1	50.8	21.8	**10.4**
	10-12	436.2	183.5	64.5	29.3	**14.9**

Data in the highlighted cells represent the minimum deviations in specific energy, corresponding to drilling at approximately the recommended optimal thrust force. When deviating from the optimal thrust value, the percentage deviation increases.

Summary and conclusion

The paper presents a new method for efficient control of small-diameter drilling of strong to very strong solid rock. It is based on accurate, reliable measurement, monitoring, and recording of thrust force and penetration depth during rock drilling with small-diameter diamond core drill bits.

For research purposes, experiments with a total drilled length of approximately 30m were carried out on a laboratory drilling rig using andesite from a local quarry as the test rock. Three diamond core drill bits commonly used for exploration purposes were tested during the experiments, differing only in the number and size of diamond grains surface-set in the bit core matrix. All experiments were performed while drilling with a constant rotation speed and a continuously increasing thrust force. The use of such unconventional drilling conditions increased bit wear and enabled us to monitor changes in the rock/bit zone over a relatively short drilled length.

As part of the research, we have reached the following findings:

- Experimental and theoretical research has allowed us to identify the key variables defining the rock drilling process. The mathematical expression of their relationships serves as the basis for models for real-time calculation of thrust force and the penetration-depth thresholds that define the drilling zone at minimum specific energy values.
- Our research has shown the simplicity of drilling optimisation in terms of specific energy based on a single controlled variable - penetration depth.
- Continuous acquisition of process variables from 116 experiments, their mathematical processing, evaluation, analysis of individual experiments, and comparison of data have shown that there are significant differences between the used drill bits in terms of thrust force required to achieve an efficient drilling zone. The lowest thrust force required for drilling at minimum specific energy is achieved with the bit equipped with larger-grained diamonds (bit 12/18), which also shows the slowest increase in effective thrust force with increasing drilled depth. A higher diamond concentration better protects the bit matrix and allows the use of a higher thrust force to ensure efficient drilling, as confirmed by the results for bits 16/25 and 25/35.
- The thrust force required for efficient rock drilling for all tested bits increased continuously with increasing drilled length, which was related to the gradual deterioration of the bit's drilling capabilities due to the diamond wear. For bit 16/25, a significant shift of the efficient drilling zone to a higher thrust force was recorded after 8 drilled meters due to its damage.
- Experimental results for all tested core bits document that the greatest penetration depth is at a thrust force that defines the upper limit of the efficient drilling zone. Drilling with this force will ensure the use of the entire interval in which the specific energy value approaches its minimum.
- The result is a flexible and adaptive optimisation algorithm for core-drilling control with surface-set diamond core drill bits. The proposed algorithm controls drilling efficiency using a single measured

quantity: penetration depth. To meet the optimisation criterion, the cyclically measured penetration depth must remain within the calculated efficient drilling zone. Drilling outside the calculated penetration depth interval will cause an estimated surge in specific energy of 10-30%. Bit wear or local changes in rock properties will initiate a new calculation of drilling parameters.

As part of the research, it was necessary to perform cost- and time-consuming experimental testing. The presented results provide a theoretical basis for efficient small-diameter drilling into strong to very strong rocks based on a single controlled variable - penetration depth. The task of our proposed optimal drilling control is to extend the drilling phase, during which the penetration depth is achieved at low energy load, by controlling interventions in the drilling regime. Thus, the specific energy serves as an optimisation parameter of the drilling process. The proposed analytical solutions used in the optimisation algorithm delivered several advantages. They relate to the reduction of the energy consumption of the drilling process and have a positive impact on increasing the bit lifetime, which will be reflected in an increase in the drilled depth, extension of the intervals of necessary service shutdowns, and ultimately reduce the costs of service, maintenance, and total operating costs of rock drilling.

References

Al-Sudani, J. A. (2017). Real-time monitoring of mechanical specific energy and bit wear using control engineering systems. *Journal of Petroleum Science and Engineering*, *149*, 171–182. doi:10.1016/J.PETROL.2016.10.038

Babaei Khorzoughi, M., & Hall, R. (2016). Processing of measurement while drilling data for rock mass characterization. *International Journal of Mining Science and Technology*, *26*(6), 989–994. doi:https://doi.org/10.1016/j.ijmst.2016.09.005

Bhatnagar, A., Khandelwal, M., & Rao, K. U. M. (2011). Laboratory Investigations for the Role of Flushing Media in Diamond Drilling of Marble. *ROCK MECHANICS AND ROCK ENGINEERING*, *44*(3), 349–356. doi:10.1007/s00603-011-0144-7

Blišťan, P. (1999). Mathematical statistics in the geology [Matematická štatistika v geológii]. Acta Montanistica Slovaca, 4(2), 115–123. https://actamont.tuke.sk/pdf/1999/n2/4blistan.pdf

Chen, X., Fan, H., Guo, B., Gao, D., Wei, H., & Ye, Z. (2014). Real-Time Prediction and Optimization of Drilling Performance Based on a New Mechanical Specific Energy Model. *Arabian Journal for Science and Engineering*, *39*(11), 8221–8231. doi:10.1007/s13369-014-1376-0

Chen, X., Gao, D., Guo, B., & Feng, Y. (2016). Real-time optimization of drilling parameters based on mechanical specific energy for rotating drilling with positive displacement motor in the hard formation. *JOURNAL OF NATURAL GAS SCIENCE AND ENGINEERING*, *35*(A), 686–694. doi:10.1016/j.jngse.2016.09.019

Davarpanah, A., Mirshekari, B., & Razmjoo, A. (2020). A parametric study to numerically analzse the formation damage effect. *ENERGY EXPLORATION \& EXPLOITATION*, *38*(2), 555–568. doi:10.1177/0144598719873094

Deng, S., Yang, S., Chi, Y., Lei, Y., Peng, H., Zhang, Y., … Wang, L. (2022). Bit optimization method for rotary impact drilling based on specific energy model. *JOURNAL OF PETROLEUM SCIENCE AND ENGINEERING*, *218*. doi:10.1016/j.petrol.2022.110977

Downton, G. C. (2012). Challenges of Modeling Drilling Systems For the Purposes of Automation and Control. *IFAC Proceedings Volumes*, *45*(8), 201–210. doi:https://doi.org/10.3182/20120531-2-NO-4020.00054

Eaton, M. J., Crivelli, D., Williams, R., & Byrne, C. (2023). Monitoring the drilling process of carbon fibre laminates using acoustic emission. *PROCEEDINGS OF THE INSTITUTION OF MECHANICAL ENGINEERS PART B-JOURNAL OF ENGINEERING MANUFACTURE*, *237*(8), 1182–1193. doi:10.1177/09544054221124474

Feng, S., Wang, Y., Zhang, G., Zhao, Y., Wang, S., Cao, R., & Xiao, E. (2020). Estimation of optimal drilling efficiency and rock strength by using controllable drilling parameters in rotary non-percussive drilling. *JOURNAL OF PETROLEUM SCIENCE AND ENGINEERING*, *193*. doi:10.1016/j.petrol.2020.107376

Flegner, P., Kačur, J., Durdán, M., & Laciak, M. (2019). Evaluating Noise Sources in a Working Environment when Disintegrating Rocks by Rotary Drilling. *Polish Journal of Environmental Studies*, *28*(5), 3711–3720. doi:10.15244/pjoes/94848

Godhavn, J.-M., Pavlov, A., Kaasa, G.-O., & Rolland, N. L. (2011). Drilling seeking automatic control solutions. *IFAC Proceedings Volumes*, *44*(1), 10842–10850. doi:https://doi.org/10.3182/20110828-6-IT-1002.00551

Guo, Y., Ren, G., Yang, F., Yang, Y., Bokov, D. O., & Fardeeva, I. N. (2021). An analytical method to select appropriate linear and non-linear correlations on the effectiveness of penetration rate parameter towards mechanical specific energy. *ENERGY REPORTS*, *7*, 3647–3654. doi:10.1016/j.egyr.2021.06.055

Hankins, D., Salehi, S., & Karbalaei Saleh, F. (2015). An Integrated Approach for Drilling Optimization Using Advanced Drilling Optimizer. *Journal of Petroleum Engineering*, *2015*, 281276.

Hassan, A., Elkatatny, S., & Al-Majed, A. (2020). Coupling rate of penetration and mechanical specific energy to Improve the efficiency of drilling gas wells. *JOURNAL OF NATURAL GAS SCIENCE AND ENGINEERING*, *83*. doi:10.1016/j.jngse.2020.103558

He, M., Li, N., Zhu, J., & Chen, Y. (2020). Advanced prediction for field strength parameters of rock using drilling operational data from impregnated diamond bit. *Journal of Petroleum Science and Engineering*, *187*, 106847. doi:10.1016/j.petrol.2019.106847

Hegde, C., Millwater, H., Pyrcz, M., Daigle, H., & Gray, K. (2019). Rate of penetration (ROP) optimization in drilling with vibration control. *Journal of Natural Gas Science and Engineering*, *67*, 71–81. doi:10.1016/j.jngse.2019.04.017

Huang, S. L., & Wang, Z. W. (1997). The mechanics of diamond core drilling of rocks. *International Journal of Rock Mechanics and Mining Sciences*, *34*(3–4), 134.e1-134.e14. doi:10.1016/S1365-1609(97)00233-5

Kalantari, S., Baghbanan, A., & Hashemalhosseini, H. (2019). An analytical model for estimating rock strength parameters from small-scale drilling data. *Journal of Rock Mechanics and Geotechnical Engineering*, *11*(1), 135–145. doi:10.1016/J.JRMGE.2018.09.005

Kalantari, S., Hashemolhosseini, H., & Baghbanan, A. (2018). Estimating rock strength parameters using drilling data. *INTERNATIONAL JOURNAL OF ROCK MECHANICS AND MINING SCIENCES*, *104*, 45–52. doi:10.1016/j.ijrmms.2018.02.013

Karakus, M., & Perez, S. (2014). Acoustic emission analysis for rock-bit interactions in impregnated diamond core drilling. *INTERNATIONAL JOURNAL OF ROCK MECHANICS AND MINING SCIENCES*, *68*, 36–43. doi:10.1016/j.ijrmms.2014.02.009

Khadisov, M., Hagen, H., Jakobsen, A., & Sui, D. (2020). Developments and experimental tests on a laboratory-scale drilling automation system. *JOURNAL OF PETROLEUM EXPLORATION AND PRODUCTION TECHNOLOGY*, *10*(2), 605–621. doi:10.1007/s13202-019-00767-6

Khosravanian, R., Sabah, M., Wood, D. A., & Shahryari, A. (2016). Weight on drill bit prediction models: Sugeno-type and Mamdani-type fuzzy inference systems compared. *JOURNAL OF NATURAL GAS SCIENCE AND ENGINEERING*, *36*(A), 280–297. doi:10.1016/j.jngse.2016.10.046

Klaic, M., Murat, Z., Staroveski, T., & Brezak, D. (2018). Tool wear monitoring in rock drilling applications using vibration signals. *WEAR*, *408*, 222–227. doi:10.1016/j.wear.2018.05.012

Krupa, V., Krul'akova, M., Lazarova, E., Labas, M., Feriancikova, K., & Ivanicova, L. (2018). Measurement, modeling and prediction of penetration depth in rotary drilling of rocks. *MEASUREMENT*, *117*, 165–175. doi:10.1016/j.measurement.2017.12.007

Lazarová, E., Kruľáková, M., Labaš, M., Ivaničová, L., & Feriančiková, K. (2020). Vibration signal for identification of concrete drilling process and drill bit wear. *Engineering Failure Analysis*, *108*. doi:10.1016/j.engfailanal.2019.104302

Li, H., Liu, S., & Chang, H. (2020). Experimental research on the influence of working parameters on the drilling efficiency. *Tunnelling and Underground Space Technology*, *95*, 103174. doi:10.1016/J.TUST.2019.103174

Lin, W., Yu, P., Zhang, C. P., & Zhang, P. (2012). *The Research Progress of Automatic Drilling Technology*. In L. C. Zhang, C. L. Zhang, J. H. Horng, & Z. Chen (Eds.), *MANUFACTURING ENGINEERING AND AUTOMATION II, PTS 1-3* (Vol. 591–593, pp. 432–435). doi:10.4028/www.scientific.net/AMR.591-593.432

Ma, S., Wu, M., Chen, L., & Lu, C. (2023). Design and application of weight-on-bit control system for drilling process: A variable-gain integrated controller with multiple-model parameter estimation. *CONTROL ENGINEERING PRACTICE*, *130*. doi:10.1016/j.conengprac.2022.105378

Meng, Y.-F., Yang, M., Li, G., Li, Y.-J., Tang, S.-H., Zhang, J., & Lin, S.-Y. (2012). New method of evaluation and optimization of drilling efficiency while drilling based on mechanical specific energy theory, *36*, 110-114+119. doi:10.3969/j.issn.1673-5005.2012.02.018

Mostofi, M., Richard, T., Franca, L., & Yalamanchi, S. (2018). Wear response of impregnated diamond bits. *WEAR*, *410*, 34–42. doi:10.1016/j.wear.2018.04.010

Oyedere, M., & Gray, K. (2020). Torque-on-bit (TOB) prediction and optimization using machine learning algorithms. *Journal of Natural Gas Science and Engineering*, *84*. doi:10.1016/j.jngse.2020.103623

Perez, S., Karakus, M., & Pellet, F. (2017a). Development of a Tool Condition Monitoring System for Impregnated Diamond Bits in Rock Drilling Applications. *ROCK MECHANICS AND ROCK ENGINEERING*, *50*(5), 1289–1301. doi:10.1007/s00603-016-1150-6

Perez, S., Karakus, M., & Pellet, F. (2017b). Development of a Tool Condition Monitoring System for Impregnated Diamond Bits in Rock Drilling Applications. *Rock Mechanics and Rock Engineering*, *50*(5), 1289–1301. doi:10.1007/s00603-016-1150-6

Pessier, R. C., & Fear, M. J. (1992). *Quantifying Common Drilling Problems With Mechanical Specific Energy and a Bit-Specific Coefficient of Sliding Friction* (Vol. All Days, p. SPE-24584-MS). doi:10.2118/24584-MS

Sakiz, U., Aydin, H., & Yarali, O. (2022). Investigation of the rock drilling performance of rotary core drilling. *BULLETIN OF ENGINEERING GEOLOGY AND THE ENVIRONMENT*, *81*(1). doi:10.1007/s10064-021-02534-6

Shishavan, R. A., Hubbell, C., Perez, H., Hedengren, J., & Pixton, D. (2015). Combined Rate of Penetration and Pressure Regulation for Drilling Optimization by Use of High-Speed Telemetry. *SPE DRILLING \& COMPLETION*, *30*(1), 17–26.

Singh, T. N., Kainthola, A., & Venkatesh, A. (2012). Correlation Between Point Load Index and Uniaxial Compressive Strength for Different Rock Types. *ROCK MECHANICS AND ROCK ENGINEERING*, *45*(2), 259–264. doi:10.1007/s00603-011-0192-z

Soares, C., & Gray, K. (2019). Real-time predictive capabilities of analytical and machine learning rate of penetration (ROP) models. *JOURNAL OF PETROLEUM SCIENCE AND ENGINEERING*, *172*, 934–959. doi:10.1016/j.petrol.2018.08.083

Tang, L., Zhu, X., Qian, X., & Shi, C. (2017). Effects of weight on bit on torsional stick-slip vibration of oilwell drill string. *JOURNAL OF MECHANICAL SCIENCE AND TECHNOLOGY*, *31*(10), 4589–4597. doi:10.1007/s12206-017-0905-7

Teale, R. (1965). The concept of specific energy in rock drilling. *International Journal of Rock Mechanics and Mining Sciences & Geomechanics Abstracts*, *2*(1), 57–73. doi:10.1016/0148-9062(65)90022-7

Wang, K., Hu, Y., Yang, K., Qin, M., Li, Y., Liu, G., & Wang, G. (2020). Experimental evaluation of rock disintegration detection in drilling by a new acoustic sensor method. *JOURNAL OF PETROLEUM SCIENCE AND ENGINEERING*, *195*. doi:10.1016/j.petrol.2020.107853

Wang, Y., & Salehi, S. (2015). Application of Real-Time Field Data to Optimize Drilling Hydraulics Using Neural Network Approach. *JOURNAL OF ENERGY RESOURCES TECHNOLOGY-TRANSACTIONS OF THE ASME*, *137*(6). doi:10.1115/1.4030847

Yassien, M. A., Sayed, M. A., Boghdady, G. Y., Ali, M. A. M., & Mohamed, A. S. (2020). *Experimental research into the effect of some operation factors and rock properties on the rate of penetration. Mining of Mineral Deposits, 14*(1), 38–43. https://doi.org/10.33271/mining14.01.036

Zhou, Y., Zhang, W., Gamwo, I., & Lin, J.-S. (2017). Mechanical specific energy versus depth of cut in rock cutting and drilling. *INTERNATIONAL JOURNAL OF ROCK MECHANICS AND MINING SCIENCES*, *100*, 287–297. doi:10.1016/j.ijrmms.2017.11.004